

# L-Histidine-Derived Smart Antifouling Biohybrid with Multistimuli Responsivity

Sk Arif Mohammad, Subrata Dolui, Devendra Kumar, Shivshankar R. Mane, and Sanjib Banerjee\*



Cite This: <https://doi.org/10.1021/acs.biomac.1c00748>



Read Online

ACCESS |



Metrics & More

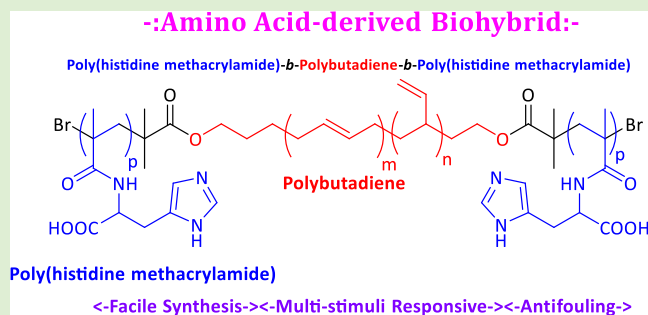


Article Recommendations



Supporting Information

**ABSTRACT:** A novel dual pH/thermoreponsive amphiphilic poly(histidine methacrylamide)-*block*-hydroxyl-terminated polybutadiene-*block*-poly(histidine methacrylamide) (PHisMAM-*b*-PB-*b*-PHisMAM) triblock copolymer biohybrid, composed of hydrophobic PB and ampholytic PHisMAM segments, is developed via direct switching from living anionic polymerization to recyclable nanoparticle catalyst-mediated reversible-deactivation radical polymerization (RDRP). The transformation involved in situ postpolymerization modification of living polybutadiene-based carbanionic species, end-capped with ethylene oxide, into dihydroxyl-terminated polybutadiene and a subsequent reaction with 2-bromo-2-methylpropionyl bromide resulting in a telechelic ATRP macroinitiator (Br-PB-Br). Br-PB-Br was used to mediate RDRP of an L-histidine-derived monomer, HisMAM, yielding a series of PHisMAM-*b*-PB-*b*-PHisMAM triblock copolymers. The copolymer's stimuli response was assessed against pH and temperature changes. The copolymer is capable of switching among its zwitterionic, anionic, and cationic forms and exhibited unique antifouling properties in its zwitterionic form. These novel triblock copolymers are expected to show promising potential in biomedical applications.



## 1. INTRODUCTION

Nature has developed several strategies utilizing the receptive properties of highly functional protein molecules to efficiently perform a variety of complex biological functions. Notably, many biological processes, including but not limited to controlled complex enzyme-mediated reactions, can be induced by temperature<sup>1</sup> or pH.<sup>2</sup> The development of novel synthetic analogues that mimic the nature's designs and are capable of responding to physical and chemical changes in their environment, such as temperature and light,<sup>3</sup> may enable new advanced applications. Covalent attachment of synthetic polymers with various biomolecules (such as poly(amino acid)/peptide/protein) affords facile access to biohybrids, which combine benefits from both the synthetic polymer world and nature.<sup>4</sup> These hybrids possess some unique properties such as excellent biodegradability and biocompatibility as well as the ability to self-assemble into well-defined three-dimensional nanostructures. Recently, these biohybrids have been attracting considerable attention for the development of environment friendly smart materials for application in engineering and biomedical sciences.<sup>5</sup> Among these, amino acid-based zwitterionic polymers<sup>6,7</sup> are very attractive to researchers as they show some unique properties such as water solubility, low toxicity, biocompatibility, and biodegradability. On the other hand, hydroxyl-terminated polybutadiene (HTPB), a low molecular weight telechelic rubber, has been used in many engineering and material applications due to its

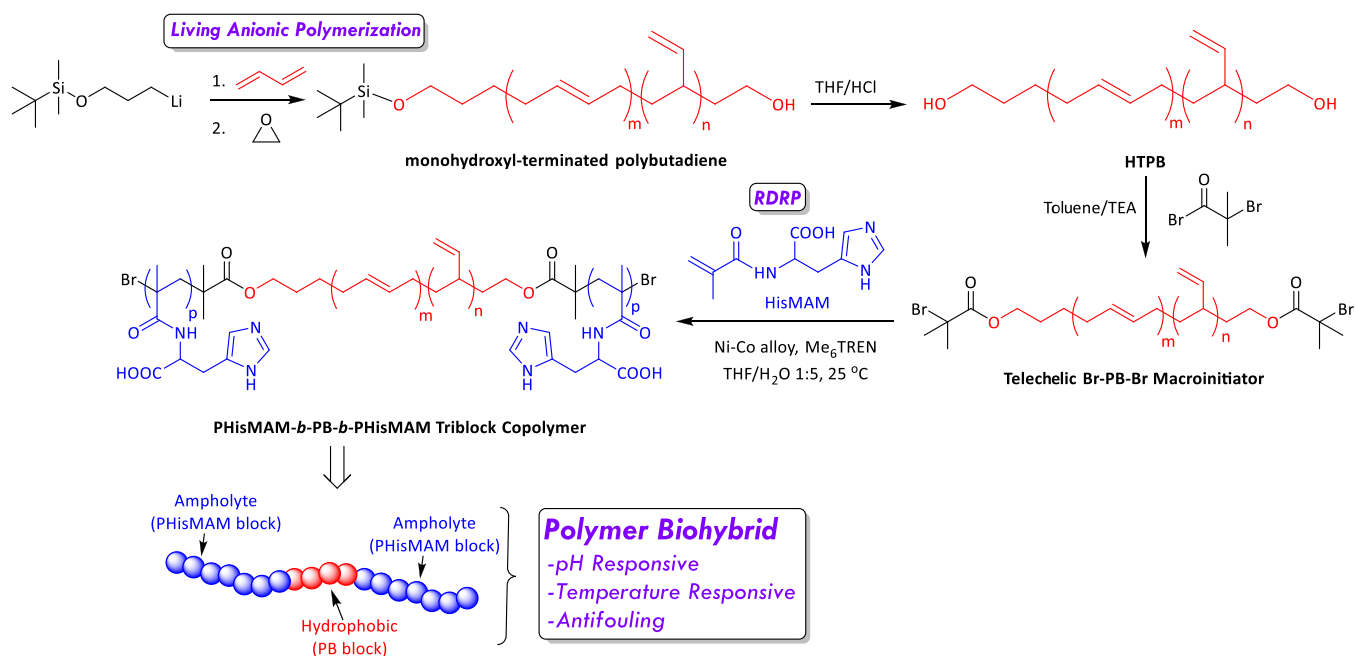
low viscosity, good transparency, oil resistance, and ease of processability.<sup>8</sup> Thus, a combination of the properties of polybutadiene with those of an amino acid-based zwitterionic polymer may lead to a biohybrid with unique properties derived from the synergy of properties of these two individual blocks.

Recent developments in the reversible-deactivation radical polymerization (RDRP) technique have revolutionized the field of precision polymer synthesis, providing access to well-defined functional (co)polymers with high end group fidelity and complex macromolecular architectures.<sup>9</sup> Some of the widely used RDRP techniques are atom transfer radical polymerization (ATRP),<sup>10–12</sup> single-electron transfer living radical polymerization (SET-LRP),<sup>13,14</sup> reversible addition–fragmentation chain transfer (RAFT) polymerization,<sup>15,16</sup> organometallic-mediated radical polymerization,<sup>17,18</sup> organo-heteroatom-mediated radical polymerization,<sup>19</sup> and nitroxide-mediated radical polymerization (NMP).<sup>20</sup> Some interesting block copolymers with unique properties have been synthe-

Received: June 11, 2021

Revised: July 17, 2021

### Scheme 1. Synthesis of PHisMAM-*b*-PB-*b*-PHisMAM Triblock Copolymer Biohybrids via Mechanistic Transformation of Living Anionic Polymerization into RDRP



sized using controlled polymerization techniques.<sup>21,22</sup> Materials with antifouling properties<sup>23–28</sup> are indispensable for a wide range of biomedical applications. Polyethylene glycol (PEG) has been the most widely used antifouling agent in biotechnology, surface science, packaging, and chemical engineering.<sup>29</sup> However, PEG is nonbiodegradable and leads to bioaccumulation.<sup>30</sup> Thus, there is a need to develop alternative antifouling materials for biotechnological and biomedical applications. Zwitterionic polymers have excellent antifouling ability and have been postulated as a new generation of antifouling materials.<sup>31</sup> To this end, researchers have developed natural amino acid (L-cysteine<sup>32,33</sup> and L-serine<sup>34</sup>)-based zwitterionic polymers that are sometimes employed to develop antifouling materials.

However, some of these materials contain toxic thiol<sup>32</sup> or synthesized via RAFT<sup>34</sup> polymerization. Also, there is a plethora of reports on the synthesis of amino acid-based polymers (which does not exhibit antifouling properties) via different RDRP techniques such as ATRP, NMP, and RAFT polymerization.<sup>35</sup> However, the synthesis of such polymers suffer from major drawbacks: (a) difficulty in recovery of the catalyst residues from the final products, which leads to their coloration and sometimes toxicity (for ATRP),<sup>36</sup> (b) undesired color, odor, and toxicity due to S-chain ends (for RAFT polymerization),<sup>37</sup> and (c) difficulty in the separation of residual Cu(I) and/or Cu(II) precursors (used for in situ generation of Cu(0) and Cu(0) from the final polymers (for SET-LRP)).<sup>38</sup> Considering the ever expanding interest in amino acid-based stimuli-responsive antifouling polymers toward applications in biological and therapeutic fields, there is a need to develop a green synthesis protocol for the construction of a novel amino acid-based multifunctional network with antifouling properties and tunable stimuli-responsive properties for applications in emerging areas.

Herein, we report for the first time the synthesis of a novel ABA-type amphiphilic dual pH/thermoreponsive poly-(histidine methacrylamide)-*block*-polybutadiene-*block*-poly-

(histidine methacrylamide) (PHisMAM-*b*-PB-*b*-PHisMAM) triblock copolymer biohybrid, composed of L-histidine (ampholyte) and butadiene (hydrophobic moiety),<sup>39</sup> via recyclable (up to multiple cycles) alloy-mediated ambient temperature RDRP of an L-histidine-derived monomer, HisMAM, using a telechelic bromo-terminated polybutadiene (Br–PB–Br) macroinitiator (Scheme 1). Br–PB–Br was synthesized via living anionic polymerization of butadiene followed by postpolymerization modification. These novel PHisMAM-*b*-PB-*b*-PHisMAM triblock copolymers are expected to show promising potential for biomedical applications and demonstrate an antifouling behavior.

## 2. EXPERIMENTAL SECTION

### 2.1. Experimental Procedures. 2.1.1. Materials.

Cobalt(II) acetylacetonate (Co(acac)<sub>2</sub>, 97%, Aldrich), nickel(II) acetylacetonate (Ni(acac)<sub>2</sub>, 95%, Aldrich), hydrazine hydrate (N<sub>2</sub>H<sub>4</sub>·H<sub>2</sub>O, reagent grade, N<sub>2</sub>H<sub>4</sub> 50–60%, Aldrich), poly(vinylphenol) (PVPPh, M<sub>w</sub> ~ 11,000, Aldrich), ethyl α-bromoisobutyrate (EBiB, 98%, Aldrich), 2-bromo-2-methylpropionyl bromide (BiBB, 98%, Aldrich), triethylamine (TEA, ≥99%, Aldrich), tris[2-(dimethylamino)ethyl]-amine (Me<sub>6</sub>TREN, >98%, TCI Chemicals), L-histidine (His, ≥99%, Aldrich), N-isopropylacrylamide (NIPAM, 99%, TCI Chemicals), poly(ethylene glycol) (PEG, M<sub>n</sub> 400, Aldrich), bovine serum albumin (BSA, ≥98.0%, Aldrich), methacryloyl chloride (Avra, India, purity 95%), 8-hydroxyquinoline (TCI Chemicals, purity >99%), sodium hydroxide (NaOH, 96%, Finar, India), sodium nitrate (NaNO<sub>3</sub>, 97%, Finar, India), potassium carbonate (K<sub>2</sub>CO<sub>3</sub>, ≥98.0%, Aldrich), sodium chloride (NaCl, 98%, Finar, India), and hydrochloric acid (HCl, 12 N, Finar, India) were used as received. Milli-Q water of specific resistivity of 18.2 MΩ cm at 25 °C was used in all the experiments. Methanol (MeOH, Merck, India), ethyl acetate (Merck, India), and ethanol (Merck, India) were purified by distillation just before use in the polymerization. Deuterium oxide (D<sub>2</sub>O) used for nuclear magnetic resonance (NMR) spectroscopy was purchased from Aldrich (purity >99.9%). Cyclohexane was purchased from Sigma-Aldrich and purified by stirring over sulfuric acid and distilled over styryl lithium. MeOH and tetrahydrofuran (THF) were purchased from Spectrochem and used without further purification.

*n*-Butyl lithium, 3-chloropropanol, styrene, *t*-butyldimethylsilyl chloride, and imidazole were purchased from Sigma-Aldrich and used as received. Butadiene was purchased from Sigma-Aldrich and purified by distillation over *n*-butyl lithium. Ethylene oxide was purchased from a local vendor and purified by distillation over *n*-butyl lithium.

**2.1.2. Purification of Reagents.** **2.1.2.1. Butadiene.** This monomer is a gas at room temperature, so it is condensed into a flask (A) that contains *n*-butyl lithium (*n*-BuLi) at  $-78\text{ }^{\circ}\text{C}$  (dry ice/isopropanol bath). The monomer is stirred for 20–30 min at  $10\text{ }^{\circ}\text{C}$  (ice/salt bath). Then, it is distilled into another flask (B) containing fresh *n*-BuLi and allowed to stand for 20–30 min at  $10\text{ }^{\circ}\text{C}$  until the viscosity is slightly increased indicating the absence of active impurities.

**2.1.2.2. Ethylene Oxide.** Ethylene oxide is a low boiling compound, and it is initially condensed into a cylinder containing freshly ground calcium hydride ( $\text{CaH}_2$ ). It was stirred over  $\text{CaH}_2$  on a vacuum line for about 30 min at  $0\text{ }^{\circ}\text{C}$  and distilled under a reduced pressure. Ethylene oxide was further distilled over *n*-BuLi using the freeze–pump–thaw technique. During its exposure to *n*-BuLi, ethylene oxide was kept at  $0\text{ }^{\circ}\text{C}$  with stirring for 30 min. Finally, the pure monomer was distilled into a graduated cylinder and stored at  $20\text{ }^{\circ}\text{C}$  until further use.

**2.1.2.3. Cyclohexane.** Purification of cyclohexane was carried out by treating with sulfuric acid for 1 week and then stirring over  $\text{CaH}_2$ . It was then degassed and distilled under vacuum in a reservoir containing *n*-BuLi with styrene as an indicator. Presence of the orange color indicates that the solvent is moisture-free and can be used for polymerization.

**2.1.3. Synthesis of Ni–Co Alloy Nanoparticles.** Ni–Co alloy nanoparticles were prepared by following a procedure reported earlier.<sup>40</sup> Typically,  $\text{Co}(\text{acac})_2$  (0.005 mol) and  $\text{Ni}(\text{acac})_2$  (0.005 mol) were added to a solution of PVPh in DMSO (0.2 wt %) under a  $\text{N}_2$  atmosphere and then  $\text{N}_2\text{H}_4 \cdot \text{H}_2\text{O}$  solution and NaOH solution (0.02 M) were added to the solution rapidly and the mixture was stirred magnetically at  $70\text{ }^{\circ}\text{C}$  for 2 h. After the reaction, the solution was allowed to cool down to room temperature and a mixture of water and ethanol (1:2 v/v) was added to it. The prepared alloy nanoparticles were isolated using a bar magnet and washed thrice with a water/ethanol mixture to remove unreacted starting materials. This purification process was repeated several times to remove the excess reactants and finally we performed drying under vacuum to obtain the Ni–Co alloy nanoparticle.

**2.1.4. Synthesis of *l*-Histidine Methacrylamide (HisMAM).** HisMAM was prepared following a modification of a procedure reported earlier.<sup>41</sup> Typically, *l*-histidine (500 mg) and  $\text{NaNO}_2$  (20 mg) were dissolved in  $\text{K}_2\text{CO}_3$  aqueous solution (3.0 mL, 5%, v/v) and the solution was cooled down to  $0\text{ }^{\circ}\text{C}$  in an ice bath. Methacryloyl chloride (400  $\mu\text{L}$ ) was added to the aqueous solution of *l*-histidine dropwise under a nitrogen atmosphere at  $0\text{--}5\text{ }^{\circ}\text{C}$ . After mixing, the reaction mixture was stirred continuously for 2 h at room temperature. After the reaction, the unreacted chemicals and byproducts were removed by extraction with ethyl acetate. The pH of the aqueous solution was adjusted to 5 by 2 N NaOH, and the product was extracted with ethanol to remove excess *l*-histidine and NaCl. The ethanol layer was then evaporated, and the product was dissolved in ethanol and precipitated in acetone. The precipitate was isolated and vacuum-dried for 12 h to obtain HisMAM.

<sup>1</sup>H NMR ( $\text{D}_2\text{O}$ )  $\delta$  (ppm) (Figure S2): 1.85 ( $\text{CH}_3\text{C}(\text{=CH}_2)$ ), 2.85–3.30 ( $-\text{CH}_2-\text{imidazole}$ ), 4.40–4.50 ( $-\text{NHCH}(\text{COOH})-\text{CH}_2-$ ), 5.40–5.60 ( $-\text{CH}_2\text{C}(\text{CH}_3)-$ ), 7.10 (1H imidazole,  $-\text{C}=\text{CHN}$ ), and 8.10 (1H imidazole,  $-\text{N}=\text{CHNH}-$ ).

**2.1.5. Synthesis of HTPB.** HTPB was prepared by following a modification of a process reported earlier.<sup>42</sup> Detailed reaction steps are described below.

**2.1.5.1. Synthesis of a Silyl-Protected Hydroxyl Group Containing a Lithium Initiator.** Step I Protection of the Hydroxyl Group of 3-Chloro-propan-1-ol

To a solution of 3-chloro-propan-1-ol (5.1 mL, 60 mmol) in 100 mL of dichloromethane, imidazole (5.3 g, 78 mmol) was added and stirred for 10 min. A solution of *t*-butyldimethylsilyl chloride (10.85 g,

7.2 mmol) in dichloromethane was added for over 10 min. The reaction mixture was stirred for 12 h at room temperature. The reaction mixture was diluted with 50 mL of dichloromethane and washed with a saturated solution of  $\text{NH}_4\text{Cl}$ . The aqueous phase was extracted with dichloromethane. The combined organic phase was washed with brine and dried over  $\text{Na}_2\text{SO}_4$ . The crude product was purified by fractional distillation to obtain 3-chloro-1-*t*-butyldimethylsilyloxy propane as a colorless liquid (yield 85%).

<sup>1</sup>H NMR ( $\text{CDCl}_3$ )  $\delta$  (ppm) (Figure S3): 0.1–0.2 ( $-\text{CH}_3$  of silyl 6H), 0.82 ( $-\text{CH}_3$  of silyl 9H), 3.8 ( $-\text{OCH}_2$ , 2H), 3.6 ( $-\text{CH}_2-\text{Cl}$ , 2H), and 1.9 ( $-\text{CH}_2-$ , 2H).

Step II *t*-Butyldimethylsilyloxy-1-propyllithium

In a 250 mL three-neck round-bottom flask equipped with a Teflon-coated stir bar, dry cyclohexane (50 mL) and freshly cut pieces of lithium (0.804 g, 0.114 mol) were added under an inert atmosphere. Then, *t*-butyldimethylsilyloxy-1-chloropropane (2.0 g, 9.1 mmol) was added dropwise at  $40\text{ }^{\circ}\text{C}$  over 30 min. Upon complete addition, the reaction mixture was heated to  $60\text{ }^{\circ}\text{C}$  and stirred for 16 h. The reaction mixture was cooled to room temperature and transferred to a Schlenk flask (yield 70%).

**2.1.5.2. Synthesis of a Monohydroxyl-Terminated Polybutadiene Polymer.** To a polymerization assembly, cyclohexane (200 mL) was transferred followed by addition of butadiene (10 g) under an ice-cold condition under constant stirring. An appropriate amount of *t*-butyldimethylsilyloxy-1-propyllithium was then transferred (1.5 g) to the above solution. The reaction mixture was then stirred at room temperature for 10 min and then at  $60\text{ }^{\circ}\text{C}$  for 2 h. A small aliquot was removed for characterization. Excess of ethylene oxide was then added by transfer and polymerization was continued for the next 2 h. An appropriate amount of MeOH was then added to the reaction mass, and it was cooled to room temperature. The HTPB polymer was then isolated by precipitation in MeOH.

<sup>1</sup>H NMR ( $\text{CDCl}_3$ )  $\delta$  (ppm) (Figure S4): 0.1–0.2 ( $-\text{CH}_3$  of silyl 6H), 0.82 ( $-\text{CH}_3$  of silyl 9H), 1.2–2.4 ( $-\text{CH}_2$  of a linear chain proton), 3.4–3.6 ( $-\text{OCH}_2$ ), 4.9–5.1 ( $-\text{CH}=\text{CH}_2$  of a vinyl proton), and 5.25–5.75 ( $-\text{CH}=\text{CH}-$  of a linear chain proton).

Degree of polymerization (DP) calculation

For the monohydroxyl-terminated polybutadiene polymer, which was subsequently converted to Br–PB–Br and used as a macro-initiator for HisMAM polymerization, the DP value was calculated using <sup>1</sup>H NMR (Figure S4) using the following equations

(A) Proton No. 1, 2's total 2 protons and its integration value is 108.37.

$$A = [108.37/2] = 54.18 \quad (1)$$

(B) Proton No. 3, 4's total 3 protons and its integration value is 12.29.

$$B = [12.29/3] = 4.09 \quad (2)$$

$$DP = [A] + [B] \quad (3)$$

$$DP = 54.18 + 4.09$$

$$DP = 58.27 \sim 58.$$

**2.1.5.3. Deprotection of the Silyl Group of the Monohydroxyl-Terminated Polybutadiene Polymer.** In a 250 mL three-neck round-bottom flask equipped with a Teflon-coated stir bar, a monohydroxyl-terminated polybutadiene polymer (15 g) and tetrahydrofuran (150 mL) were added. Concentrated HCl (7 mL) was added dropwise to the above solution under stirring. The reaction was continued for the next 2 h. The reaction mixture was concentrated to 30%, and the polymer was isolated by precipitation in MeOH. Precipitation was repeated for two times and MeOH was removed by decantation. The polymer was dried under vacuum for 3 h.

<sup>1</sup>H NMR ( $\text{CDCl}_3$ )  $\delta$  (ppm) (Figure S5): 1.2–2.4 ( $-\text{CH}_2$  of a linear chain proton), 3.4–3.6 ( $-\text{OCH}_2$ , 4H), 4.9–5.1 ( $-\text{CH}=\text{CH}_2$  of a vinyl proton), and 5.25–5.75 ( $-\text{CH}=\text{CH}-$  of a linear chain proton).

**2.1.6. Synthesis of the Telechelic Br–PB–Br Macroinitiator.** The Br–PB–Br macroinitiator was prepared by modification of a process

**Table 1. Reaction Conditions and Molecular Characterization Data of PHisMAM-*b*-PB-*b*-PHisMAM Triblock Copolymers<sup>a</sup>**

entry	polymer	[HisMAM] <sub>0</sub> /[Br-PB-Br] <sub>0</sub>	conv. <sup>b</sup> (%)	<i>M</i> <sub>n,theo</sub> <sup>c</sup> (g mol <sup>-1</sup> )	<i>M</i> <sub>n,SEC</sub> <sup>d</sup> (g mol <sup>-1</sup> )	<i>Đ</i> <sup>d</sup>	<i>T</i> <sub>CP</sub> <sup>e</sup> (°C)
P1	PHisMAM <sub>50</sub> - <i>b</i> -PB <sub>58</sub> - <i>b</i> -PHisMAM <sub>50</sub>	100: 58	71	19,300	18,600	1.20	31
P2	PHisMAM <sub>100</sub> - <i>b</i> -PB <sub>58</sub> - <i>b</i> -PHisMAM <sub>100</sub>	200: 58	63	31,600	32,200	1.20	37
P3	PHisMAM <sub>150</sub> - <i>b</i> -PB <sub>58</sub> - <i>b</i> -PHisMAM <sub>150</sub>	300: 58	65	46,900	44,900	1.18	42
P4	PHisMAM <sub>200</sub> - <i>b</i> -PB <sub>58</sub> - <i>b</i> -PHisMAM <sub>200</sub>	400: 58	60	57,000	55,300	1.19	49

<sup>a</sup>Reaction conditions: solvent = THF/H<sub>2</sub>O (1: 5); catalyst = Ni-Co alloy; ligand = Me<sub>6</sub>TREN; temperature = 25 °C; and time = 24 h.

<sup>b</sup>Determined gravimetrically based on the monomer feed. <sup>c</sup>Calculated using yield as conversion and the following equation:  $M_{n,theo} = ([\text{HisMAM}]_0/[\text{Br-PB-Br}]_0 \times \text{yield} \times M_{\text{HisMAM}}) + M_{\text{Br-PB-Br}}$ , where  $M_{\text{HisMAM}} (= 223 \text{ g mol}^{-1})$  and  $M_{\text{Br-PB-Br}} (= 3500 \text{ g mol}^{-1})$  are the molecular weights of HisMAM and Br-PB-Br, respectively. <sup>d</sup>Obtained from SEC measurements. <sup>e</sup>*T*<sub>CP</sub> measured by turbidimetry.

reported earlier.<sup>43</sup> HTPB (1.37 g, 0.448 mmol) and triethylamine (147 μL, 1.056 mmol) were dissolved in anhydrous THF (38 mL) in a round-bottom flask under a N<sub>2</sub> atmosphere, and the mixture was allowed to cool down to 0 °C. Then, BiBB (120 μL, 0.968 mmol) was added dropwise to that reaction mixture under a N<sub>2</sub> atmosphere at 0 °C. The reaction mixture was stirred magnetically at 0 °C for 2 h and then at an ambient temperature for another 24 h. After this, the reaction mixture was filtered to remove the present triethylammonium bromide salt and the filtrate was then evaporated using a rotary evaporator to concentrate the reaction mixture. The concentrated solution was then precipitated in chilled MeOH. The precipitate was then dried under vacuum for 6 h at 40 °C to obtain the product, which was characterized by NMR spectroscopy.

<sup>1</sup>H NMR (CDCl<sub>3</sub>) δ (ppm) (Figure 2a): 1.22 (methylene protons in -CH<sub>2</sub>-CH-CH=CH<sub>2</sub>), 1.39 (methylene signals in -CH<sub>2</sub>-CH-CH=CH<sub>2</sub>), 1.99 (methylene signals in -CH<sub>2</sub>-CH=CH-CH<sub>2</sub>- repeating units and methyl protons -(CH<sub>3</sub>)<sub>2</sub>C(Br) in bromo-initiator residues), 3.10 (-CH<sub>2</sub>, signal g), 5.38 (methylene proton signals -CH=CH- in the *cis/trans*-1,4 olefinic structure), and 5.54 (alkenyl proton signals -CH=CH<sub>2</sub> in the 1,2-vinyl-terminated structure).

**2.1.7. Syntheses of PHisMAM-*b*-PB-*b*-PHisMAM Triblock Copolymers.** The syntheses of PHisMAM-*b*-PB-*b*-PHisMAM triblock copolymers were carried out using Br-PB-Br as the macroinitiator under a N<sub>2</sub> atmosphere using Schlenk techniques. Typically, the Br-PB-Br macroinitiator, Ni-Co nanoparticles, Me<sub>6</sub>TREN, and degassed THF were taken in a flask under a nitrogen flow and stirred magnetically and degassed by N<sub>2</sub> bubbling for 20 min. Then, degassed HisMAM solution in water was introduced into the flask under a nitrogen flow, and the reaction mixture was heated at 25 °C under constant stirring for 24 h. The polymerization reaction was stopped at different time intervals to estimate the monomer conversion (by gravimetry) and the molar mass (*M*<sub>n</sub>s) and dispersity values (*Đ*s) (by size-exclusion chromatography (SEC)). After completion of the reaction, the crude product was dissolved in water and the Ni-Co alloy catalyst was separated simply by holding a magnetic bar at the wall of the flask. The crude product was then precipitated in prechilled MeOH (×3 times) and filtered. The precipitate was isolated and dried under vacuum for 6 h at 40 °C and characterized by NMR spectroscopy and SEC.

<sup>1</sup>H NMR (D<sub>2</sub>O) δ (ppm) (Figure 2b, P1, Table 1): 1.08 (-CH<sub>2</sub>C(CH<sub>3</sub>) of the HisMAM repeating unit), 1.22 (methylene protons in -CH<sub>2</sub>-CH-CH=CH<sub>2</sub>), 1.40 (-CH<sub>2</sub>C(CH<sub>3</sub>) of the HisMAM repeating unit), 1.99 (methylene signals in -CH<sub>2</sub>-CH=CH-CH<sub>2</sub>- repeating units and methyl protons -(CH<sub>3</sub>)<sub>2</sub>C(Br) in bromo-initiator residues), 3.20 (-CH<sub>2</sub>CH(COOH) of the HisMAM repeating unit), 4.60 (-CH(COOH)CH<sub>2</sub> of the HisMAM repeating unit), 3.80 (-CH<sub>2</sub>, signal g), 5.38 (methylene proton signals -CH=CH- in the *cis/trans*-1,4 olefinic structure), 5.54 (methylene proton signals -CH=CH<sub>2</sub> in the 1,2-vinyl-terminated structure), 7.28 (-NH of the HisMAM repeating unit), and 7.32–7.52 (SH of the aromatic ring of the HisMAM repeating unit).

Degree of polymerization (DP) calculation

For the PHisMAM-*b*-PB-*b*-PHisMAM (P1–P4, Table 1), using <sup>1</sup>H NMR spectroscopy,

$$DP_{n,M} = \frac{\int_{4.3}^{4.6} -\text{CH}(\text{COOH})\text{CH}_2 \text{ (signal } c')}{\frac{1}{2} \times \int_{3.6}^{4.0} -\text{CH}_2 \text{ (signal } g)} \times DP_{n,\text{Br-PB-Br}} \quad (4)$$

**2.2. pH Titration.** An aqueous solution of the copolymer (0.1 M) was prepared using deionized water. The pH of the solution was adjusted to pH 1.2 using HCl. This solution was titrated against 0.25 N NaOH solution until the pH reached 12.6. During the titration, the change of pH of the solution was monitored using a pH meter.

**2.3. Antifouling Study.** Typically, 1.5 mL of aqueous solution of the polymer (1 mg mL<sup>-1</sup>) was mixed with 1.5 mL of aqueous BSA solution (1 mg mL<sup>-1</sup>) of pH 7 at 25 °C in a cuvette. The evolution of the hydrodynamic diameter of the solution with time was monitored using dynamic light scattering (DLS).

**2.4. Characterization.** **2.4.1. NMR Spectroscopy.** <sup>1</sup>H NMR spectra of the synthesized polymers were recorded at 25 °C using a Bruker 400 MHz spectrometer.

**2.4.2. Attenuated Total Reflection Infrared (ATR-IR) Spectroscopy.** The spectra were recorded using a PerkinElmer Spectrum 100 in the ATR mode with a diamond crystal using 16 scans per spectrum and a resolution of 4 cm<sup>-1</sup> and a spectral range of 4000–600 cm<sup>-1</sup>.

**2.4.3. Size Exclusion Chromatography (SEC).** *M*<sub>n</sub> and *Đ* values of the polymers were determined using a SEC with a triple-detection GPC (from Agilent Technologies) using a PL0390-0605390 LC light scattering detector capable of detecting two diffusion angles (15 and 90°), a PL0390-06034 capillary viscometer, a 390-LC PL0390-0601 refractive index detector, and two PL1113-6300 ResiPore 300 mm × 7.5 mm columns. DMF (containing 0.1 wt % of LiCl) was used as the eluent at a flow rate of 0.8 mL min<sup>-1</sup>. The entire SEC-HPLC system was thermostated at 35 °C, and narrow linear poly(methyl methacrylate) standards were used to calibrate the SEC instrument. The results were processed using the corresponding Agilent software.

**2.5. UV-vis Spectroscopy.** The thermosensitivity of the PHisMAM-*b*-PB-*b*-PHisMAM copolymer solution was measured using a Shimadzu UV-2600 spectrophotometer equipped with a temperature-controlled sample holder. A 1.0 wt % solution of PHisMAM-*b*-PB-*b*-PHisMAM in water was taken in a 3 mL quartz cuvette and placed in a UV-vis spectrophotometer equipped with a temperature controller. The transmittance of the copolymer solution was monitored at a detection wavelength of 500 nm at a heating rate of 1 °C min<sup>-1</sup> in the temperature range of 10 to 80 °C.

**2.6. Dynamic Light Scattering (DLS).** The hydrodynamic diameter (*D*<sub>h</sub>) of the aqueous solutions of the copolymers was measured using a Malvern particle size analyzer (Zetasizer NANO ZS90).

### 3. RESULTS AND DISCUSSION

**3.1. Synthesis of PHisMAM-*b*-PB-*b*-PHisMAM Triblock Copolymer Biohybrids.** The L-histidine-derived monomer, HisMAM, was prepared via a simple reaction between L-histidine with methacryloyl chloride (see Experimental Section for the detailed procedure, Scheme S1) and characterized by IR and NMR spectroscopies (see Supporting Information, Figures S1,S2). The telechelic dibromo-terminated polybuta-

diene (Br–PB–Br) macroinitiator was prepared via living anionic polymerization of butadiene, followed by end capping and postpolymerization modification (Scheme 1) and characterized by NMR spectroscopy (see Supporting Information, Figures S3–S5) and SEC (Figure 1). The  $^1\text{H}$  NMR

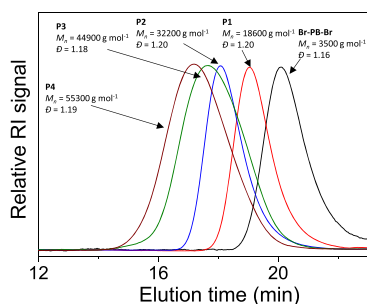


**Figure 1.** Evolution of SEC traces of the Br–PB–Br macroinitiator and PHisMAM-*b*-PB-*b*-PHisMAM triblock copolymers (P1–P4, Table 1).

spectrum of Br–PB–Br (Figure 2a) shows characteristic signals at 1.22 (methylene protons in  $-\text{CH}_2-\text{CH}=\text{CH}=\text{CH}_2$ ), 1.99 (methylene signals in  $-\text{CH}_2-\text{CH}=\text{CH}-\text{CH}_2-$  repeating units and methyl protons  $-(\text{CH}_3)_2\text{C}(\text{Br})$  in bromo-initiator residues), 5.38 (methyne proton signals  $-\text{CH}=\text{CH}-$  in the *cis/trans*-1,4 olefinic structure), and 5.54 (alkenyl proton signals  $-\text{CH}=\text{CH}_2$  in the 1,2-vinyl-terminated structure).<sup>44</sup>

A range of PHisMAM-*b*-PB-*b*-PHisMAM triblock copolymer syntheses (P1–P4, Table 1) was carried out via recyclable alloy-mediated RDRP using Br–PB–Br as the macroinitiator (Scheme 1). The SEC analysis revealed successful synthesis of the well-defined PHisMAM-*b*-PB-*b*-PHisMAM triblock copolymers (Figure 1), showing little or no starting Br–PB–Br macroinitiator. The presence of characteristic signals of the PB<sup>43,44</sup> central block and the PHisMAM<sup>45</sup> terminal block in the  $^1\text{H}$  NMR (Figure 2b) and IR spectrum (Figure S6)

confirms the product structure. The  $^1\text{H}$  NMR spectrum of PHisMAM-*b*-PB-*b*-PHisMAM (Figure 2b) reveals emergence of new signals at 1.08 ( $-\text{CH}_2\text{C}(\text{CH}_3)$  of the HisMAM repeating unit), 1.40 ( $-\text{CH}_2\text{C}(\text{CH}_3)$  of the HisMAM repeating unit), 3.20 ( $-\text{CH}_2\text{CH}(\text{COOH})$  of the HisMAM repeating unit), 4.60 ( $-\text{CH}(\text{COOH})\text{CH}_2$  of the HisMAM repeating unit), 7.28 ( $-\text{NH}$  of the HisMAM repeating unit), and 7.32–7.52 ( $^5\text{H}$  of the aromatic ring of the HisMAM repeating unit).<sup>45</sup>

Kinetic studies suggested the controlled nature of the polymerization, as proven by the pseudo-first-order kinetic plot and linear evolution of  $M_n$  with monomer conversion, retaining low  $D$  values (Figure 3). From the slope of Figure 3a, the apparent propagation rate constant  $k_{p(\text{app})}$  was determined to be  $1.6 \times 10^{-5} \text{ s}^{-1}$ .

Recyclability of the catalyst is an important characteristic of heterogeneous catalysis. Thus, to prove the ease of catalyst recyclability, the alloy catalyst was isolated just by using a bar magnet after completion of the polymerization and used for the next polymerization reaction. Results (Table S1) revealed that there is not any appreciable reduction in the catalyst efficiency (both pertaining to the control of the RDRP process and the molecular weight parameters of the prepared triblock copolymers) even after four polymerization cycles.

**3.2. pH and Temperature Response of PHisMAM-*b*-PB-*b*-PHisMAM Triblock Copolymer Biohybrids.** The pH response of the copolymer (Figure 4) revealed that the L-histidine-derived copolymer, PHisMAM-*b*-PB-*b*-PHisMAM, existed in three different charged states<sup>27</sup> depending on the pH of the solution. At low pH conditions ( $\text{pH} < 1.8$ ), both carboxylate and imidazole groups were protonated, leading to a monocationic state of the PHisMAM-*b*-PB-*b*-PHisMAM copolymer. At high pH values ( $\text{pH} > 7.1$ ), both the carboxylate and imidazole groups were deprotonated and the copolymer existed in its monoanionic state. At an intermediate pH range (between pH 1.8 and 7.1), the carboxylate groups were

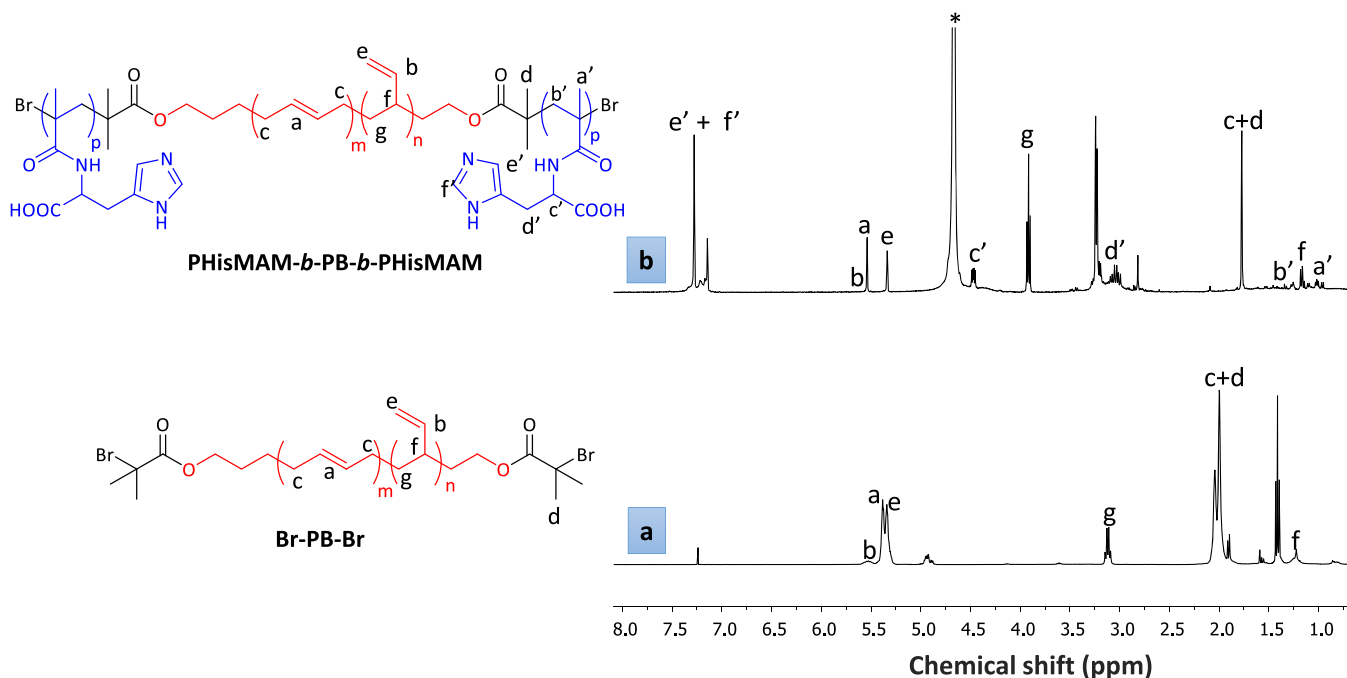


**Figure 2.**  $^1\text{H}$  NMR spectra for (a) Br–PB–Br (in  $\text{CDCl}_3$ ) and PHisMAM-*b*-PB-*b*-PHisMAM (P1, Table 1) (in  $\text{D}_2\text{O}$ ).

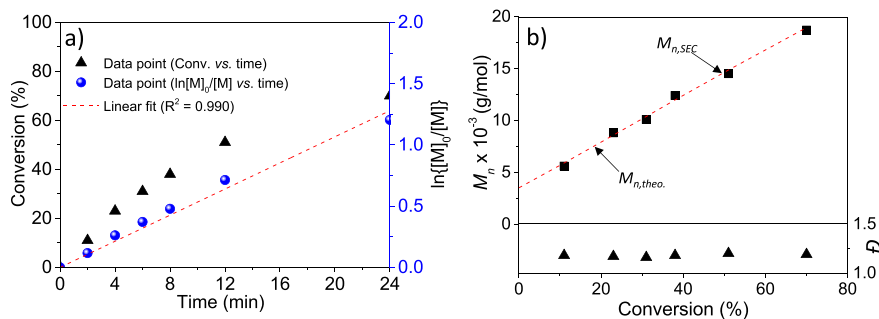


**Figure 3.** Plot of (a) conversion versus time,  $\ln([M]_0/[M])$  versus time, and (b) evolution of  $M_n$  and  $\bar{D}$  with increasing monomer conversion for alloy-mediated RDRP of HisMAM in THF/H<sub>2</sub>O 1:5 at 25 °C using Br–PB–Br as the initiator.

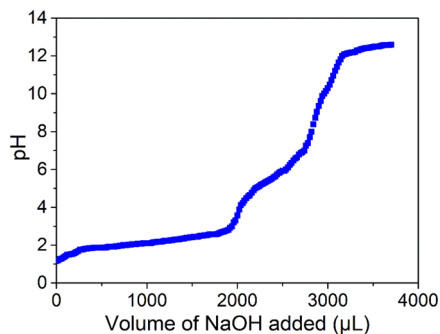


**Figure 4.** pH titration curve for the PHisMAM-*b*-PB-*b*-PHisMAM copolymer for a pH range of 1.2 to 12.6.

deprotonated and the imidazole groups were protonated, leading to the zwitterionic state of the copolymer. These pH-tunable charged states of the copolymer can be utilized for antifouling and other physical properties. Notably, throughout all pH ranges, the copolymers were not observed to aggregate and remained as unimers, as revealed by a  $D_h$  of <5 nm.

The synthesized amphiphilic PHisMAM-*b*-PB-*b*-PHisMAM triblock copolymers exhibited an unprecedented dual temperature response, whereas neither HTPB nor PHisMAM was thermoresponsive. The cloud point ( $T_{CP}$ ) of the PHisMAM-*b*-PB-*b*-PHisMAM copolymers, as determined by turbidimetry, increased with an increase of hydrophilic PHisMAM segments in the copolymer (Table 1 and Figure 5).

The origin and variation of  $T_{CP}$  as a function of the HisMAM content in the copolymer might be explained as follows. Below the lower critical solution temperature (LCST), water molecules form H-bonds with the pendent amide functionalities of the copolymer, giving it a coil conformation, which remains soluble in water. Above the LCST, enough

thermal energy is present to break the polymer–water H-bonds. Subsequently, the copolymer forms H-bonds with itself via amide and –COOH functionalities, resulting in a coil to globule transition. With the increase of the HisMAM mol % in the copolymer, the LCST increases as there are more amide functionalities present to form H-bonds with water molecules, making the copolymer soluble until sufficient thermal energy is provided.

The effect of pH on the LCST of the copolymer was measured using PHisMAM<sub>50</sub>-*b*-PB<sub>58</sub>-*b*-PHisMAM<sub>50</sub> as the representative sample. At pH 7.0, the LCST of the copolymer (P1, Table 1) was approximately 31 °C. When pH of the solution was adjusted to 1.5 and 10.5, in both cases, the LCST increased to 35 and 41 °C, respectively. This is probably due to the fact that the copolymer in its cationic (at pH 1.5) or anionic (at pH 10.5) state has higher solubility in water due to the enhanced hydrophilicity of the polymer chain compared to its zwitterionic state (at pH 7.0).

**3.3. Antifouling Behavior of PHisMAM-*b*-PB-*b*-PHisMAM Triblock Copolymer Biohybrids.** The pH titration (Figure 4) revealed that the PHisMAM-*b*-PB-*b*-PHisMAM copolymer existed in its zwitterionic form in the pH ranges of 1.8–7.1. Zwitterionic polymers in aqueous solution have the ability to strongly bind to H<sub>2</sub>O molecules via electrostatically induced hydration and thus demonstrate antifouling performance.<sup>46</sup> Compared to PEG,<sup>29</sup> the most widely used antifouling material, which is nonbiodegradable and leads to bioaccumulation,<sup>30</sup> zwitterionic polymers offer a broader chemical diversity and greater freedom for molecular design and may emerge as a degradable, nonbioaccumulate alternative to PEG for the development of antifouling materials suitable for biomedical applications.<sup>47</sup>

In order to investigate the antifouling nature in solutions, the resistivity of BSA, as a representative protein, was tested

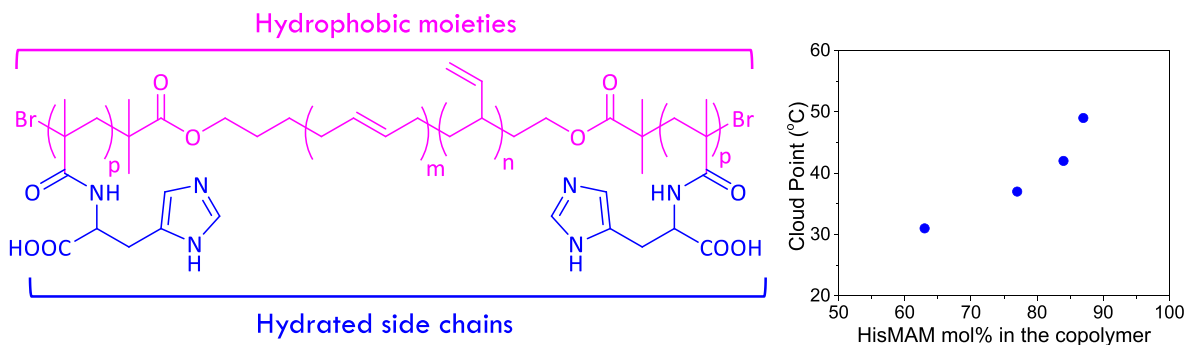


**Figure 5.**  $T_{CP}$  as a function of the HisMAM content in PHisMAM-*b*-PB-*b*-PHisMAM triblock copolymers at pH 7.0.

toward the PHisMAM-*b*-PB-*b*-PHisMAM copolymer and the result was compared with a representative fouling polymer (PNIPAM)<sup>48</sup> and an antifouling polymer (PEG) (see [Experimental Section](#) for more details). The  $D_h$  of the solution mixture containing the polymer (PHisMAM-*b*-PB-*b*-PHisMAM or PNIPAM or PEG) and BSA was estimated by DLS at different time intervals at pH 7 with the assumption that a fouling polymer will allow aggregation of the polymer leading to an increase of the  $D_h$  while an antifouling polymer will not allow any fouling and the  $D_h$  will remain the same with time. The results ([Figure 6](#)) revealed that  $D_h$  of the solution

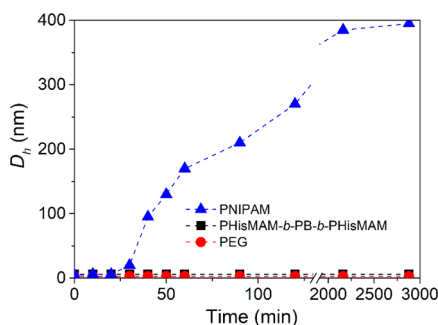


**Figure 6.** Variation of the hydrodynamic diameters of the aqueous solutions of PNIPAM, PEG, and PHisMAM-*b*-PB-*b*-PHisMAM in the presence of BSA at 25 °C.

increased for PNIPAM, indicating fouling and formation of aggregates via hydrophobic interactions of BSA with PNIPAM. However, when PEG or PHisMAM-*b*-PB-*b*-PHisMAM was used, the  $D_h$  value remained the same even after 48 h, suggesting the absence of any fouling. This result indicated that PHisMAM-*b*-PB-*b*-PHisMAM offers significant resistance toward protein adsorption and may be useful for the preparation of an antifouling surface and employed as an alternative to PEG. Notably, all the copolymers (P1–P4, [Table 1](#)) exhibited an antifouling behavior only at their zwitterionic state (at pH 7). None of these copolymers exhibited the antifouling behavior in their cationic form. This is in accordance with the other amino acid-derived polymers that exhibited the antifouling behavior only at their zwitterionic state.<sup>31–34</sup> The copolymer exhibited the antifouling behavior even when higher concentrations of BSA (3 and 5 mg mL<sup>-1</sup>) were used. Notably, control samples, poly(histidine methacrylamide) (PHisMAM) and poly(lysine methacrylamide) (PLysMAM), in their zwitterionic state, exhibited an antifouling behavior against BSA. The  $D_h$  value remained the same as that at time  $t = 0$  even after 48 h.

#### 4. CONCLUSIONS

In summary, we report, for the very first time, synthesis of a novel amphiphilic PHisMAM-*b*-PB-*b*-PHisMAM triblock copolymer composed of L-histidine (ampholyte) and butadiene (hydrophobic moiety) via mechanistic transformation from living anionic polymerization into recyclable alloy-mediated RDRP. This new class of novel biohybrid allows the integration of functionalities of two different blocks (a synthetic polymer and a biomolecule). The synthesized zwitterionic copolymer is capable of switching among zwitterionic, anionic, and cationic forms, exhibiting dual (pH and temperature) stimuli-responsive properties and reducing adsorption of proteinase. The collective advantages of ease of

catalyst synthesis, handling, recovery, reusability, and protecting group-free chemistry may allow wide applicability of this facile synthesis protocol for the synthesis of biohybrids for application in some promising areas including biomedical science and materials science. The synthesized multistimuli-responsive antifouling biohybrid may be useful for the construction of a multistimuli-responsive actuator for biomedical applications.

#### ■ ASSOCIATED CONTENT

##### Supporting Information

The Supporting Information is available free of charge at <https://pubs.acs.org/doi/10.1021/acs.biomac.1c00748>.

Catalyst recyclability study, synthesis of HisMAM, and ATR-IR and NMR spectra of compounds ([PDF](#))

#### ■ AUTHOR INFORMATION

##### Corresponding Author

Sanjib Banerjee – Department of Chemistry, Indian Institute of Technology Bhilai, Raipur 492015 Chhattisgarh, India; [orcid.org/0000-0003-4841-4408](https://orcid.org/0000-0003-4841-4408); Email: [sanjib.banerjee@iitbhilai.ac.in](mailto:sanjib.banerjee@iitbhilai.ac.in)

##### Authors

Sk Arif Mohammad – Department of Chemistry, Indian Institute of Technology Bhilai, Raipur 492015 Chhattisgarh, India; [orcid.org/0000-0002-2162-4416](https://orcid.org/0000-0002-2162-4416)  
 Subrata Dolui – Department of Chemistry, Indian Institute of Technology Bhilai, Raipur 492015 Chhattisgarh, India  
 Devendra Kumar – Department of Chemistry, Indian Institute of Technology Bhilai, Raipur 492015 Chhattisgarh, India; [orcid.org/0000-0003-0354-1489](https://orcid.org/0000-0003-0354-1489)  
 Shivshankar R. Mane – Polymer Science and Engineering Division, CSIR-National Chemical Laboratory, Pune, Maharashtra 411008, India; [orcid.org/0000-0003-3853-449X](https://orcid.org/0000-0003-3853-449X)

Complete contact information is available at: <https://pubs.acs.org/10.1021/acs.biomac.1c00748>

##### Notes

The authors declare no competing financial interest.

#### ■ ACKNOWLEDGMENTS

We appreciate financial support from the Science and Engineering Research Board, India through the Ramanujan Fellowship Award (SB/S2/RJN-113/2016) and the Early Career Research Award (ECR/2018/001990) and IIT Bhilai for the Research Initiation Grant. S.A.M. and D.K. thank the MHRD, Govt. of India and CSIR, Govt. of India for their fellowships, respectively. S.R.M. thank the CSIR-SRA (Scientist's Pool Scheme, Award No. 13(9139-A)/2020-Pool) for the funding. We would like to thank Prof. Tarun K. Mandal (Indian Association for the Cultivation of Science), Dr. P. P. Wadgaonkar (CSIR-NCL), and Dr. A. V. Ambade (CSIR-NCL) for fruitful discussions.

#### ■ REFERENCES

- (1) Lindquist, S.; Craig, E. A. The Heat-Shock Proteins. *Annu. Rev. Genet.* **1988**, *22*, 631–677.
- (2) Perutz, M. Electrostatic Effects in Proteins. *Science* **1978**, *201*, 1187–1191.

- (3) Wei, M.; Gao, Y.; Li, X.; Serpe, M. J. Stimuli-Responsive Polymers and Their Applications. *Polym. Chem.* **2017**, *8*, 127–143.
- (4) Liu, X.; Gao, W. Precision Conjugation: An Emerging Tool for Generating Protein–Polymer Conjugates. *Angew. Chem., Int. Ed.* **2021**, *60*, 11024–11035.
- (5) Chen, C.; Ng, D. Y. W.; Weil, T. Polymer Bioconjugates: Modern Design Concepts toward Precision Hybrid Materials. *Prog. Polym. Sci.* **2020**, *105*, No. 101241.
- (6) Banerjee, S.; Maji, T.; Paira, T. K.; Mandal, T. K. Amino-Acid-Based Zwitterionic Polymer and Its Cu(II)-Induced Aggregation into Nanostructures: A Template for CuS and CuO Nanoparticles. *Macromol. Rapid Commun.* **2013**, *34*, 1480–1486.
- (7) Mohammad, S. A.; Dolui, S.; Kumar, D.; Alam, M. M.; Banerjee, S. Anisotropic and Self-Healing Copolymer with Multiresponsive Capability via Recyclable Alloy-Mediated RDRP. *Macromol. Rapid Commun.* **2021**, *42*, No. 2100096.
- (8) Chaturvedi, S.; Dave, P. N. Solid Propellants: AP/HTPB Composite Propellants. *Arab. J. Chem.* **2019**, *12*, 2061–2068.
- (9) Bagheri, A.; Fellows, C. M.; Boyer, C. Reversible Deactivation Radical Polymerization: From Polymer Network Synthesis to 3D Printing. *Adv. Sci.* **2021**, *8*, No. 2003701.
- (10) Ouchi, M.; Terashima, T.; Sawamoto, M. Transition Metal-Catalyzed Living Radical Polymerization: Toward Perfection in Catalysis and Precision Polymer Synthesis. *Chem. Rev.* **2009**, *109*, 4963–5050.
- (11) Matyjaszewski, K. Atom Transfer Radical Polymerization (ATRP): Current Status and Future Perspectives. *Macromolecules* **2012**, *45*, 4015–4039.
- (12) Saha, A.; Paira, T. K.; Biswas, M.; Jana, S.; Banerjee, S.; Mandal, T. K. Combined atom-transfer radical polymerization and ring-opening polymerization to design polymer–polypeptide copolymer conjugates toward self-aggregated hybrid micro/nanospheres for dye encapsulation. *J. Polym. Sci. Part A: Polym. Chem.* **2015**, *53*, 2313–2319.
- (13) Anastasaki, A.; Nikolaou, V.; Nurumbetov, G.; Wilson, P.; Kempe, K.; Quinn, J. F.; Davis, T. P.; Whittaker, M. R.; Haddleton, D. M. Cu(0)-Mediated Living Radical Polymerization: A Versatile Tool for Materials Synthesis. *Chem. Rev.* **2016**, *116*, 835–877.
- (14) Lligadas, G.; Grama, S.; Percec, V. Single-Electron Transfer Living Radical Polymerization Platform to Practice, Develop, and Invent. *Biomacromolecules* **2017**, *18*, 2981–3008.
- (15) Moad, G. RAFT Polymerization to form Stimuli-Responsive Polymers. *Polym. Chem.* **2017**, *8*, 177–219.
- (16) Banerjee, S.; Patil, Y.; Gimello, O.; Ameduri, B. Well-defined multiblock poly(vinylidene fluoride) and block copolymers thereof: a missing piece of the architecture puzzle. *Chem. Commun.* **2017**, *53*, 10910–10913.
- (17) Demarteau, J.; Debuigne, A.; Detrembleur, C. Organocobalt Complexes as Sources of Carbon-Centered Radicals for Organic and Polymer Chemistries. *Chem. Rev.* **2019**, *119*, 6906–6955.
- (18) Banerjee, S.; Ladmiral, V.; Debuigne, A.; Detrembleur, C.; Rahaman, S. M. W.; Poli, R.; Ameduri, B. Organometallic-Mediated Alternating Radical Copolymerization of tert-Butyl-2-Trifluoromethylacrylate with Vinyl Acetate and Synthesis of Block Copolymers Thereof. *Macromol. Rapid Commun.* **2017**, *38*, No. 1700203.
- (19) Yamago, S. Precision Polymer Synthesis by Degenerative Transfer Controlled/Living Radical Polymerization using Organotellurium, Organostibine, and Organobismuthine Chain-Transfer Agents. *Chem. Rev.* **2009**, *109*, 5051–5068.
- (20) Nicolas, J.; Guillaneuf, Y.; Lefay, C.; Bertin, D.; Gimes, D.; Charleux, B. Nitroxide-Mediated Polymerization. *Prog. Polym. Sci.* **2013**, *38*, 63–235.
- (21) Que, Y.; Liu, Y.; Tan, W.; Feng, C.; Shi, P.; Li, Y.; Xiaoyu, H. Enhancing Photodynamic Therapy Efficacy by Using Fluorinated Nanoplatfrom. *ACS Macro Lett.* **2016**, *5*, 168–173.
- (22) Tao, D.; Feng, C.; Cui, Y.; Yang, X.; Manners, I.; Winnik, M. A.; Huang, X. Monodisperse Fiber-like Micelles of Controlled Length and Composition with an Oligo(p-phenylenevinylene) Core via “Living” Crystallization-Driven Self-Assembly. *J. Am. Chem. Soc.* **2017**, *139*, 7136–7139.
- (23) Xu, B.; Feng, C.; Hu, J.; Shi, P.; Gu, G.; Wang, L.; Huang, X. Spin-Casting Polymer Brush Films for Stimuli-Responsive and Anti-Fouling Surfaces. *ACS Appl. Mater. Interfaces* **2016**, *8*, 6685–6692.
- (24) Xu, B.; Liu, Y.; Sun, X.; Hu, J.; Shi, P.; Huang, X. Semifluorinated Synergistic Nonfouling/Fouling-Release Surface. *ACS Appl. Mater. Interfaces* **2017**, *9*, 16517–16523.
- (25) Feng, C.; Huang, X. Polymer Brushes: Efficient Synthesis and Applications. *Acc. Chem. Res.* **2018**, *51*, 2314–2323.
- (26) Ishii, T.; Wada, A.; Tsuzuki, S.; Casolaro, M.; Ito, Y. Copolymers Including l-Histidine and Hydrophobic Moiety for Preparation of Nonbiofouling Surface. *Biomacromolecules* **2007**, *8*, 3340–3344.
- (27) Wang, H.; Wu, H.; Lee, C.-J.; Lei, X.; Zhe, J.; Xu, F.; Cheng, F.; Cheng, G. pH-Sensitive Poly(histidine methacrylamide). *Langmuir* **2016**, *32*, 6544–6550.
- (28) Casolaro, M.; Bottari, S.; Ito, Y. Vinyl Polymers Based on l-Histidine Residues. Part 2. Swelling and Electric Behavior of Smart Poly(ampholyte) Hydrogels for Biomedical Applications. *Biomacromolecules* **2006**, *7*, 1439–1448.
- (29) Arami, H.; Khandhar, A.; Liggitt, D.; Krishnan, K. M. In Vivo Delivery, Pharmacokinetics, Biodistribution and Toxicity of Iron Oxide Nanoparticles. *Chem. Soc. Rev.* **2015**, *44*, 8576–8607.
- (30) Garay, R. P.; El-Gewely, R.; Armstrong, J. K.; Garratty, G.; Richette, P. Antibodies against polyethylene glycol in healthy subjects and in patients treated with PEG-conjugated agents. *Expert Opin. Drug Delivery* **2012**, *9*, 1319–1323.
- (31) Chang, Y.; Chen, S.; Yu, Q.; Zhang, Z.; Bernards, M.; Jiang, S. Development of Biocompatible Interpenetrating Polymer Networks Containing a Sulfobetaine-Based Polymer and a Segmented Polyurethane for Protein Resistance. *Biomacromolecules* **2007**, *8*, 122–127.
- (32) Rosen, J. E.; Gu, F. X. Surface Functionalization of Silica Nanoparticles with Cysteine: A Low-Fouling Zwitterionic Surface. *Langmuir* **2011**, *27*, 10507–10513.
- (33) Azari, S.; Zou, L. Fouling Resistant Zwitterionic Surface Modification of Reverse Osmosis Membranes using Amino Acid L-Cysteine. *Desalination* **2013**, *324*, 79–86.
- (34) Liu, Q.; Singh, A.; Liu, L. Amino Acid-Based Zwitterionic Poly(serine methacrylate) as an Antifouling Material. *Biomacromolecules* **2013**, *14*, 226–231.
- (35) Bauri, K.; Nandi, M.; De, P. Amino Acid-Derived Stimuli-Responsive Polymers and Their Applications. *Polym. Chem.* **2018**, *9*, 1257–1287.
- (36) Boyer, C.; Corrigan, N. A.; Jung, K.; Nguyen, D.; Nguyen, T.-K.; Adnan, N. N. M.; Oliver, S.; Shanmugam, S.; Yeow, J. Copper-Mediated Living Radical Polymerization (Atom Transfer Radical Polymerization and Copper(0) Mediated Polymerization): From Fundamentals to Bioapplications. *Chem. Rev.* **2016**, *116*, 1803–1949.
- (37) Nurumbetov, G.; Engelis, N.; Godfrey, J.; Hand, R.; Anastasaki, A.; Simula, A.; Nikolaou, V.; Haddleton, D. M. Methacrylic Block Copolymers by Sulfur Free RAFT (SF RAFT) Free Radical Emulsion Polymerisation. *Polym. Chem.* **2017**, *8*, 1084–1094.
- (38) Rosen, B. M.; Jiang, X.; Wilson, C. J.; Nguyen, N. H.; Monteiro, M. J.; Percec, V. The Disproportionation of Cu(I)X Mediated by Ligand and Solvent Into Cu(0) And Cu(II)X<sub>2</sub> and Its Implications for SET-LRP. *J. Polym. Sci. Part A: Polym. Chem.* **2009**, *47*, 5606–5628.
- (39) Lauterbach, F.; Rubens, M.; Abetz, V.; Junkers, T. Ultrafast PhotoRAFT Block Copolymerization of Isoprene and Styrene Facilitated through Continuous-Flow Operation. *Angew. Chem., Int. Ed.* **2018**, *57*, 14260–14264.
- (40) Raula, M.; Rashid, M. H.; Lai, S.; Roy, M.; Mandal, T. K. Solvent-Adoptable Polymer Ni/NiCo Alloy Nanochains: Highly Active and Versatile Catalysts for Various Organic Reactions in both Aqueous and Nonaqueous Media. *ACS Appl. Mater. Interfaces* **2012**, *4*, 878–889.

- (41) Abd-Rabboh, H. S.; Kamel, A. H. Mimicking a receptor for cyanide ion based on ion imprinting and its applications in potential transduction. *Electroanalysis* **2012**, *24*, 1409–1415.
- (42) Lee, I.; Bates, F. S. Synthesis, Structure, and Properties of Alternating and Random Poly(styrene-*b*-butadiene) Multiblock Copolymers. *Macromolecules* **2013**, *46*, 4529–4539.
- (43) Luo, Y.-L.; Yang, X.-L.; Xu, F.; Chen, Y.-S.; Zhao, X. pH-triggered PMAA-*b*-HTPB-*b*-PMAA Copolymer Micelles: Physicochemical Characterization and Camptothecin Release. *Colloid Polym. Sci.* **2014**, *292*, 1061–1072.
- (44) Fang, T. Characterization of a Carboxyl-Terminated Butadiene-Acrylonitrile Copolymer by Two-Dimensional Nuclear Magnetic Resonance. *Macromolecules* **1990**, *23*, 2145–2152.
- (45) Odaba, M.; Garipcan, B.; Dede, S.; Denizli, A. Methacrylamidohistidine in Affinity Ligands for Immobilized Metal-Ion Affinity Chromatography of Human Serum Albumin. *Biotechnol. Bioprocess Eng.* **2001**, *6*, 402.
- (46) Mi, L.; Jiang, S. Integrated Antimicrobial and Nonfouling Zwitterionic Polymers. *Angew. Chem., Int. Ed.* **2014**, *53*, 1746–1754.
- (47) Liu, N.; Han, J.; Zhang, X.; Yang, Y.; Liu, Y.; Wang, Y.; Wu, G. pH-responsive Zwitterionic Polypeptide as a Platform for Anti-Tumor Drug Delivery. *Colloid. Surf. B* **2016**, *145*, 401–409.
- (48) Lanzaalaco, S.; Armelin, E. Poly(N-isopropylacrylamide) and Copolymers: A Review on Recent Progresses in Biomedical Applications. *Gels* **2017**, *3*, 36.